SEISMIC CHARACTERIZATION OF NORTHEAST ASIA

Kevin G. Mackey[1], Hans E. Hartse[2], Lee K, Steck[2], Richard J. Stead[2], Charlotte A. Rowe[2], Kazuya Fujita[1], and Luiza Gutirrez[1]

Michigan State University[1] and Los Alamos National Laboratory[2]

Sponsored by the National Nuclear Security Administration
Office of Nonproliferation Research and Development
Office of Defense Nuclear Nonproliferation

Contract Nos. DE-FC52-2004NA25540[1] and DE-AC52-06NA25396[2]

ABSTRACT

Our project of seismic characterization of northeast Asia continues on a multi-faceted approach concentrating on eastern Russia. The field work aspects of the project have included temporary station deployments, new permanent seismic station installations, and calibration of existing digital stations. Seismic station deployments include a 5 station temporary deployment in the Stanovoi Range in southern Yakutia/northern Amur region and two stations deployed in the vicinity of Yakutsk. The station deployments in the Stanovoi Range investigated the connection between a young volcanic field and a large cluster of poorly located historical seismicity and were the first ever seismic deployments in that region of eastern Russia. The volcanic field appears to be aseismic although surrounding areas were found to be very active, with more than 20 locatable local events per day recorded. We also mapped large scale active thrust faults in the region, which combined with observed seismicity will help us understand expected seismicity patterns, location quality, and tectonic models. We also are working on establishing 2 permanent stations in the Amur region and continue to work on station calibrations, with recent data acquired at Stekolnyi.

Our Siberia database enhancements for this past year include (1) addition of new earthquakes and explosions and associated phase data, amplitudes, etc., primarily from the Irkutsk, Yakutsk, and Magadan networks for the years 1999-2006; (2) additions of amplitude data primarily from the Chukotka and Amur regions to aid amplitude tomography efforts; and (3) general quality control efforts primarily targeting unmerged, multi-author origins, the resolution of duplicated arrival information, and the inclusion of United States Geological Survey Earthquake Data Reports (USGS EDR) and International Seismological Centre (ISC) magnitudes for larger events where Russian network operators did not report a K-class or a magnitude estimate.

We have been performing Pn and Pg tomography to obtain average crustal and upper mantle velocities in northeast Asia. Pn velocities are higher beneath the Siberian Platform and generally lower under the tectonically active regions in the central and eastern portions of our study area. Pg velocities show a similar geographic trend, and our results agree closely with Pg results from earlier studies. Pg velocities beneath Sakhalin Island are anomalously low, and we are working to understand this observation. Travel time correction surfaces will be developed from the tomographic maps, and these will be compared to correction surfaces currently being developed from the raw travel time data.

We are using catalog amplitude parameters to derive a two-dimensional (2-D) function that maps laterally varying attenuation features. We are using selected Pg and Sg amplitude readings from the Siberia database. We derive the 2-D attenuation mapping using tomographic methods and compare our results with known tectonic and seismic velocity perturbation features derived in previous work.

We have continued our explosion discrimination work with the current focus on data obtained by our deployed digital stations over the period 2000-2006. We have examined amplitude ratios and find similar results to those previously obtained using analog records. The best results are obtained using full vector ratios, which results in correct event identification as high as 82%.

OBJECTIVES

The main objective of our current research is to improve the overall seismic characterization of northeastern Asia. To accomplish this we seek to develop a complete seismicity database and use this database to discriminate industrial explosions, develop velocity models, and understand the relationship between the sizes and locations of events.

RESEARCH ACCOMPLISHED

Characterization of Seismicity in the Stanovoi Volcanic Field Region

The Stanovoi region of southern Yakutia is one of the most poorly understood seismically active regions in eastern Russia. Although a considerable number of earthquakes have been located in the region (Figures 1 and 2), the epicenters are poor as only regional stations located fairly far away were used in the locations. In addition, the active faults in the region and type of faulting are unknown. The levels of microseismicity are also unknown as no seismic stations have ever been deployed within several hundred kilometers. Within the Stanovoi region, a province of Cenozoic basaltic volcanism (0.5-1.0 ma) exists that is in the general vicinity of a cluster of previously located earthquakes. It has been previously unknown if the seismicity has any connection to the volcanic field or to apparent faults visible in the topography of the region. In addition, the proposed Russian extension of the Tanlu fault from China may terminate in the vicinity of the Stanovoi Range (Mackey et al., 2003). In this study we conducted a temporary deployment of 5 broadband seismic stations encircling the Stanovoi volcanic field in an attempt to characterize the area and gain insight into the many questions of the area.

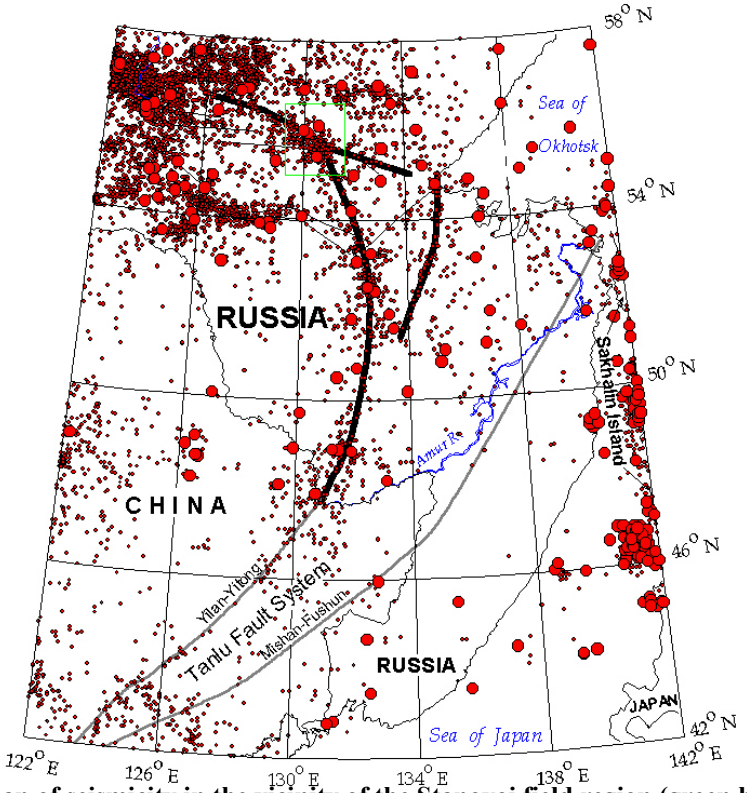

Figure 1. Index map of seismicity in the vicinity of the Stanovoi field region (green box). The heavy black line indicates possible extension of the Tanlu fault into Russia from China. In the vicinity of the Stanovoi region, it intersects a large generally east-west fault system (also heavy line) that is clearly visible on topographic maps and satellite images, but essentially unstudied. Figure modified from Mackey et al., 2003.

Station Deployments

Five broadband seismometers and digital recorders were deployed by helicopter on 12 August 2006 in the vicinity of the Stanovoi volcanic field (Figure 2). Typical station installation included digging a post hole for the instrument and burying it for thermal and wind isolation (Figure 3). Two stations were powered by batteries and solar panels, which were hampered by nearly continuous rain and poor weather starting August 13. These stations operated intermittently over about 20 days of the deployment portion of the experiment. One of these two stations was destroyed by a bear on about 23-24 August (Figure 3). Three stations were powered by large batteries. Two of these stations failed early (operating 5 and 12 days respectively) due to drained batteries. The third battery powered station was destroyed by a bear on 16 August.

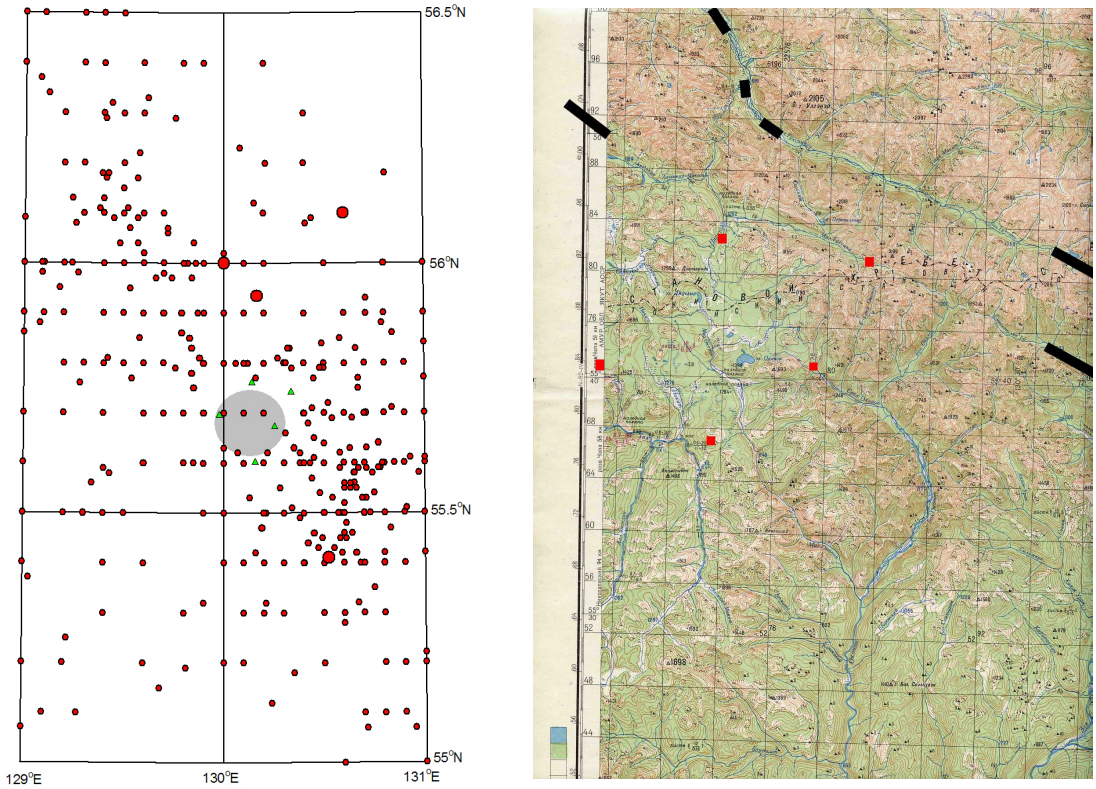

Figure 2. Left - Historic seismicity of the Stanovoi volcanic field region (approximately the grey circle). Events larger than magnitude 4.0 are shown as larger. Stations deployed as a part of this study are shown as green triangles. Note that the epicenters scatter nearly everywhere, with a slight concentration to the southeast of the volcanic field. Right - Topographic map of the Stanovoi deployment region. Stations are shown with red squares. The two eastern stations were destroyed by bears. Black bars indicate linear trends interpreted to be faults. Extensive thrust fault scarps were visible in the southern valley wall of the southern valley near the western edge of this map. The region of the Stanovoi volcanic field generally encompasses the region encircled by the seismic stations. Grid lines on this map are spaced at 4-km intervals.

Volcanic Field and Fault Lineations

Topographic maps of the Stanovoi volcanic field region indicate two large parallel linear features generally striking east-west immediately to the north of the volcanic field (Figure 2). These have previously been interpreted as strike-slip faults based on their linearity. However, in the process of deploying to the field area by helicopter, we traveled along the southern of the two valleys. In the southern side of the valley, approximately 20-40 km west of the deployed station sites, there are extensive young fault scarps on the side of the valley. The scarps are very well defined in places and are clearly southward dipping thrust faults (Figure 4). The scarps and thrust fault shown are poorly documented in the literature. There is also evidence of strike-slip faulting along the northern sides of both the northern and southern lineations. Collectively, this may indicate a region of complex tectonics.

Figure 3. Left - Typical station installation consisting of a Geotech Instruments KS-2000 broadband seismometer, Smart24 digitizer, and large battery. Right – A seismic station shown as found after destruction by a bear. The bear removed all station coverings and batteries and extracted the seismometer from its posthole.

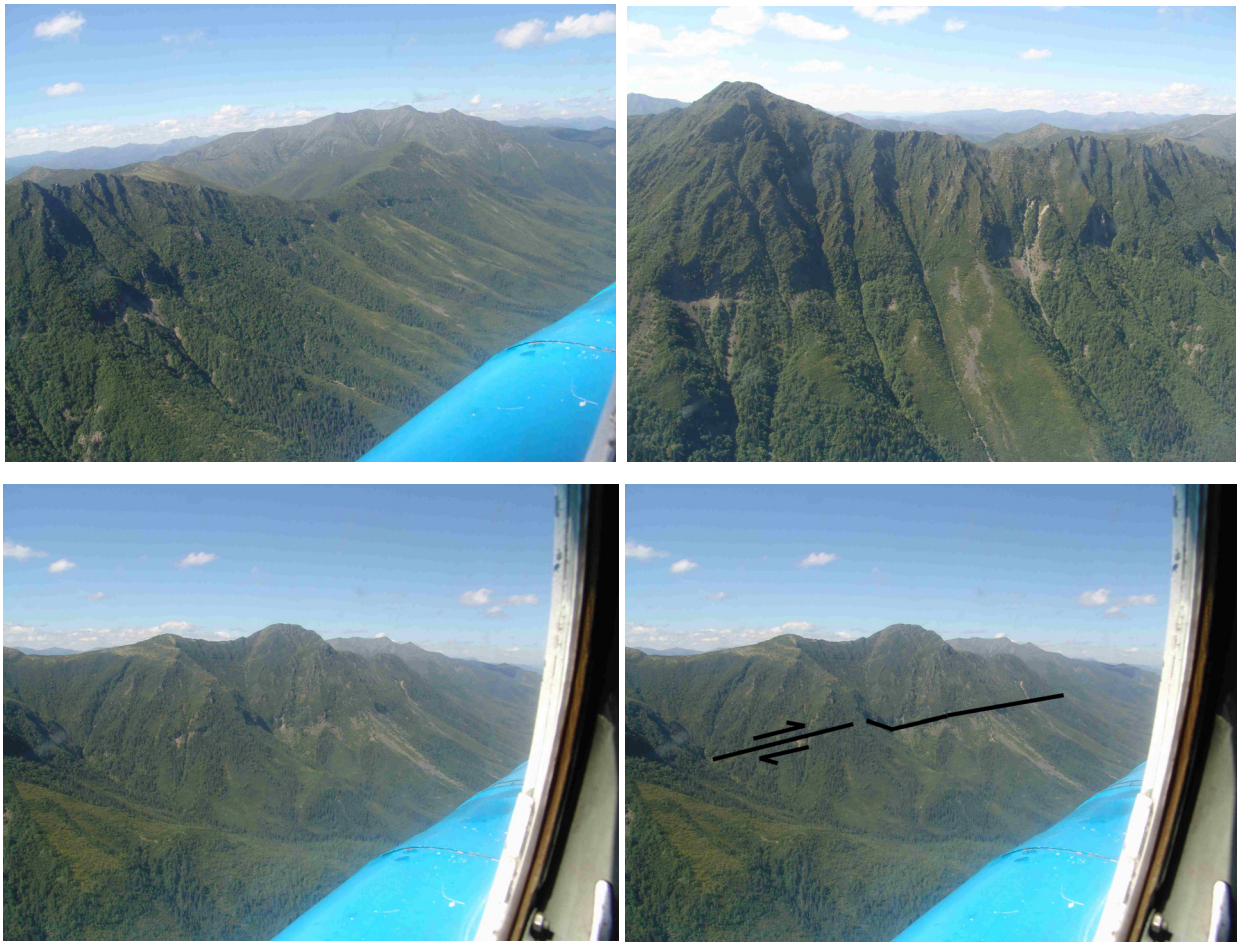

Figure 4. Upper—Photos of a well defined fault scarp visible along the southern wall of the southern linear valley (Figure 2, right) just west of the Stanovoi volcanic field. Lower—Interpretation of the same fault scarp as a thrust where the plunging dip is apparent in a side valley.

Seismicity

Although we experienced difficulty with some equipment and station destruction by bears, the situation was compensated for by higher levels of seismicity than was expected. Analysis of five days of seismic data revealed approximately 100 locatable earthquakes occurring within 50 km of the deployed stations (Figure 5) and many additional events at greater distances. A review of remaining data when only 1 or 2 stations were operating indicated many additional events. Most events are found to occur in localized clusters immediately to the southeast of the deployed network. The events located in the vicinity of the volcanic field range in magnitude from a maximum of about 2.7 down to less than 0.0. Note that there is no evidence of any type of aftershock sequence being recorded here. It is interesting to note that no events have yet been found that occur within the boundaries of the volcanic field, which thus far appears quiescent. With a couple exceptions, the events all occur to the south of the presumed strike-slip faults, consistent with the southern side being underlain by an active thrust. Depths of the locatable earthquakes are generally ranging between 9 and 15 km. An image of seismograms showing several events is in Figure 6.

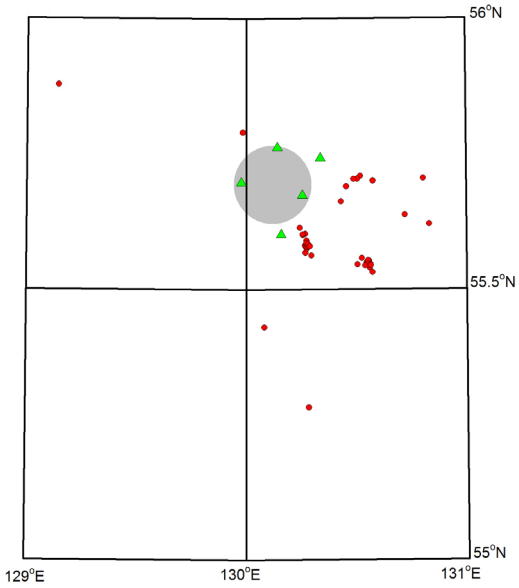

Figure 5. Locations of earthquakes recorded during the first four days of network deployment (red). Deployed stations shown as green triangles. Note that most events occur to the south and east of the stations, and no events are found that have occurred within the Stanovoi volcanic field (grey circle).

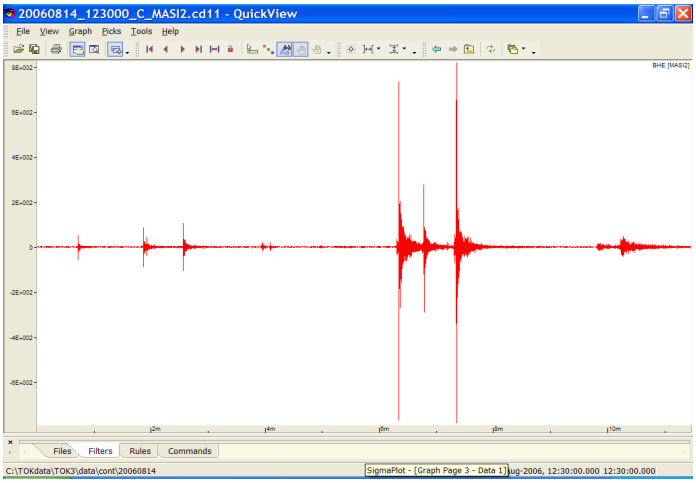

Figure 6. Image of multiple earthquakes of varying distances occurring within minutes of each other. These events occurred on September 14, 2006.

Stanovoi Study Conclusions

We have conducted the first targeted seismicity characterization study in the vicinity of the Stanovoi Range and the young Stanovoi volcanic field. Previously it was unknown if seismicity in the immediate vicinity was associated with the volcanic field. From the seismicity data and geological observations while in the field, we can make several basic conclusions for seismic characterization of the area: 1) The Stanovoi Range is more seismically active than was previously understood. 2) There appears to be no seismic activity associated with the Stanovoi volcanic field, thus explosive volcanic events are not to be expected. 3) The area may be dominated by north-south convergence and thrusting and, given the extent of visible scarps, the region may be expected to generate large earthquakes.

Database Expansion

We added about 17,000 new events to our database, with most additions coming from the Irkutsk, Yakutsk, and Magadan networks for the years 1999-2007 (Figure 7). Our total event count is now over 250,000, with over 342,000 distinct origins tied to the events. These new events also included about 100,000 new arrival times, bringing our total arrival count to about 1.44 million. Michigan State University (MSU) provided additional amplitude values from hardcopy bulletins for the Chukotka and Amur regions to provide improved ray coverage for ongoing tomography projects (see Rowe et al., these Proceedings, and Zhang et al., these Proceedings). Between new bulletins and the supplemental amplitude values we added about 60,000 new entries to our database, bringing the total amplitude count to near 690,000. For some larger events (about M > 6.0), Russian networks operators did not provide K-class or magnitude estimates. For these events, we are now obtaining magnitude values from the Los Alamos National Laboratory (LANL) global database, typically reported by the ISC or the USGS. Finally, we spent time merging some distinct origins into single events, and we corrected some origin time and arrival time data entry errors, which typically involved typos for hours, minutes, or seconds in our original bulletins.

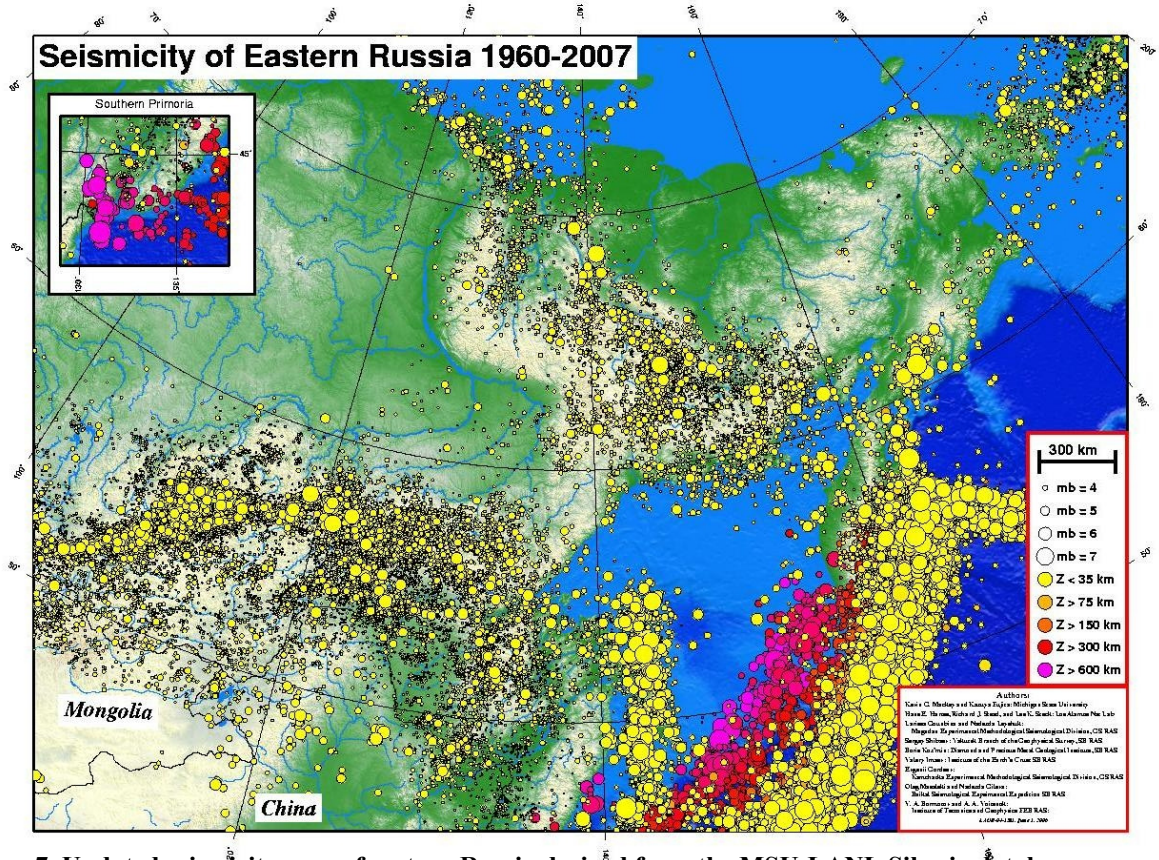

Figure 7. Updated seismicity map of eastern Russia derived from the MSU-LANL Siberia database.

Tomography

Results of crustal Pg phase velocity tomography and Lg attenuation tomography may be found in the paper by Rowe et al., these Proceedings. This work was conducted in part under this contract. Related work performed under a different contract is presented in Zhang et al., these Proceedings.

Digital Waveform Explosion Discrimination

Amplitude Discrimination

We have expanded our explosion discrimination research. Our previous work investigated explosion discrimination using amplitude data reported in the historic Russian seismic bulletins, which were derived from analog records. The methodology and results for the analog data discrimination are presented in Mackey et al. (2006) and Linkimer (2006). We apply the same methodology here to investigate Pg/Sg ratio discriminants using digital seismograms. We analyzed 34 explosion waveforms and 211 earthquake waveforms, picking amplitudes for all components of Pg and Sg waves. The digital waveforms analyzed were all within the Magadan region and recorded short period seismometers (3 components) stations, with the exception of data from Seimchan, recording broadband STS-1 instruments; thus it is possible to compare results of the analog and new digital studies. Following our previous methodology, we calculated 5 Pg/Sg ratios varying by component (Pg_z/Sg_z, Pg_h/Sg_h, Pg_z/Sg_h, Pg_h/Sg_z, and full vector Pg/Sg). We have not yet calculated network averaged ratios with the analog data, as additional stations need to be analyzed.

Comparing results of analog data discrimination (Mackey et al., 2006; Linkimer, 2006) with new digital data results, we find that we achieve better results using digital data, with generally a 10-12% improvement. In both cases, full vector Pg/Sg ratios discriminate best (Figure 8), and Pg_h/Sg_z are worst (Table 1). We also note that the critical values obtained for discriminating explosions are 2-3 times larger (depending on ratio) or higher for the digital data than the analog data (note that the critical value is the Pg/Sg ratio value that best discriminates explosions from earthquakes). It is unclear why the critical values differ between digital and analog data. Application of critical values derived from analog data is not transportable to digital data even though the seismometers used are identical (Table 1, column 4).

Table 1. Comparison of event discrimination results between analog and digital data for the Magadan region of eastern Russia.

Raw Phase Ratio	Analog Results (Mackey et al., 2006; Linkimer, 2006)		Digital Results		Results of Analog Critical Value Applied to Digital Data
Discriminant	% Events Correctly Classified	Critical Value	% Events Correctly Classified	Critical Value	% Events Correctly Classified
Pg_h/Sg_h	70.7%	0.23	80.7%	0.55	59.8%
Pg_z/Sg_z	63.8%	0.33	80.5%	0.88	65.5%
Pg_h/Sg_z	62.8%	0.48	73.9%	0.83	68.8%
Pg_z/Sg_h	67.0%	0.18	79.5%	0.62	58.3%
Full Vector	70.9%	0.27	82.4%	0.41	63.3%

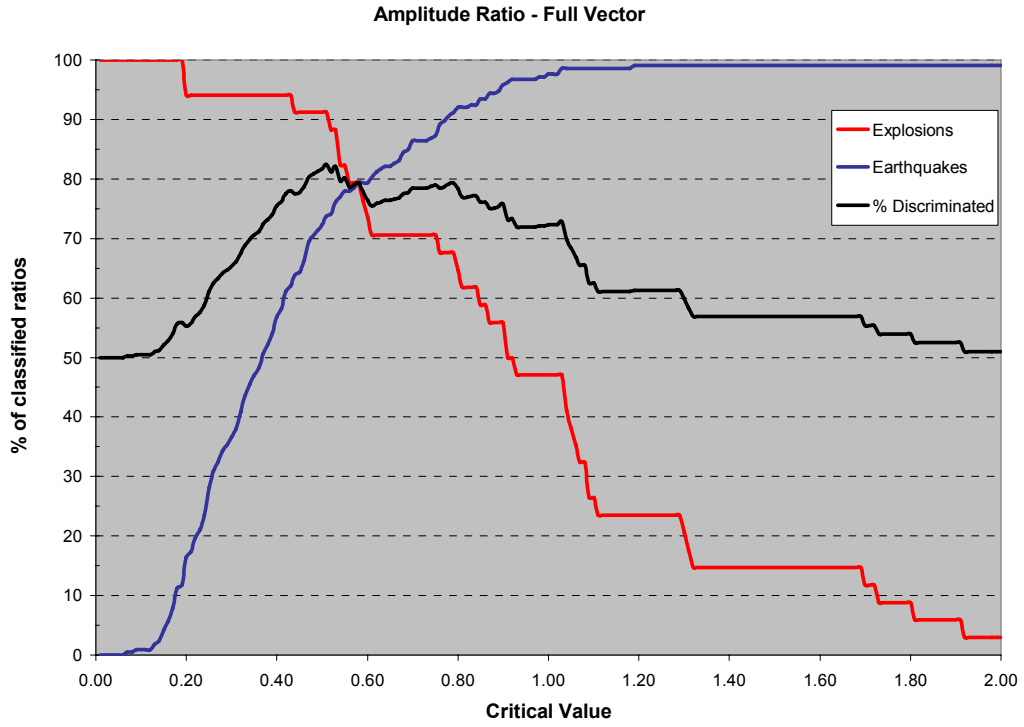

Figure 8. Full vector Pg/Sg ratio critical value determination for discriminating explosions from earthquakes using digital data from the Magadan region, eastern Russia.

Spectral Discrimination

Many of the mining explosions that take place in eastern Russia are ripple fire explosions in surface or open pit mines. Most mines in this area fire lines with a 50-ms delay. In effect, this generates a 20 Hz signal in the ground that appears to be characteristic of the regions mine explosions when the spectral amplitudes are compared to earthquakes. Figure 9 compares the typical spectral amplitude of a mine explosion to an earthquake of a similar size and distance. Note that the explosion has a spectral amplitude peak in the 18-20 Hz range, which is absent on the earthquake spectrum. It is unclear why the spectral amplitude peak of the explosions occurs slightly below the expected 20 Hz, though it may be a result of delays being slightly greater than the presumed 50 ms. The spectral peak is visible using just the P wave or S wave, or the entire waveform and is apparent on all components. Additional research is needed to develop a viable discrimination methodology using this technique.

CONCLUSIONS

The research performed here has significant implications for the interpretation of seismicity and tectonics in the Amur District, where there is significant contamination of the seismicity catalogs by industrial explosions and where the present-day tectonics are poorly understood. This will affect interpretation of tomographic models of the region (e.g., Zhang et al., this volume) and similar studies as they are extended into the even less well-known Magadan and northeastern Yakutian regions.

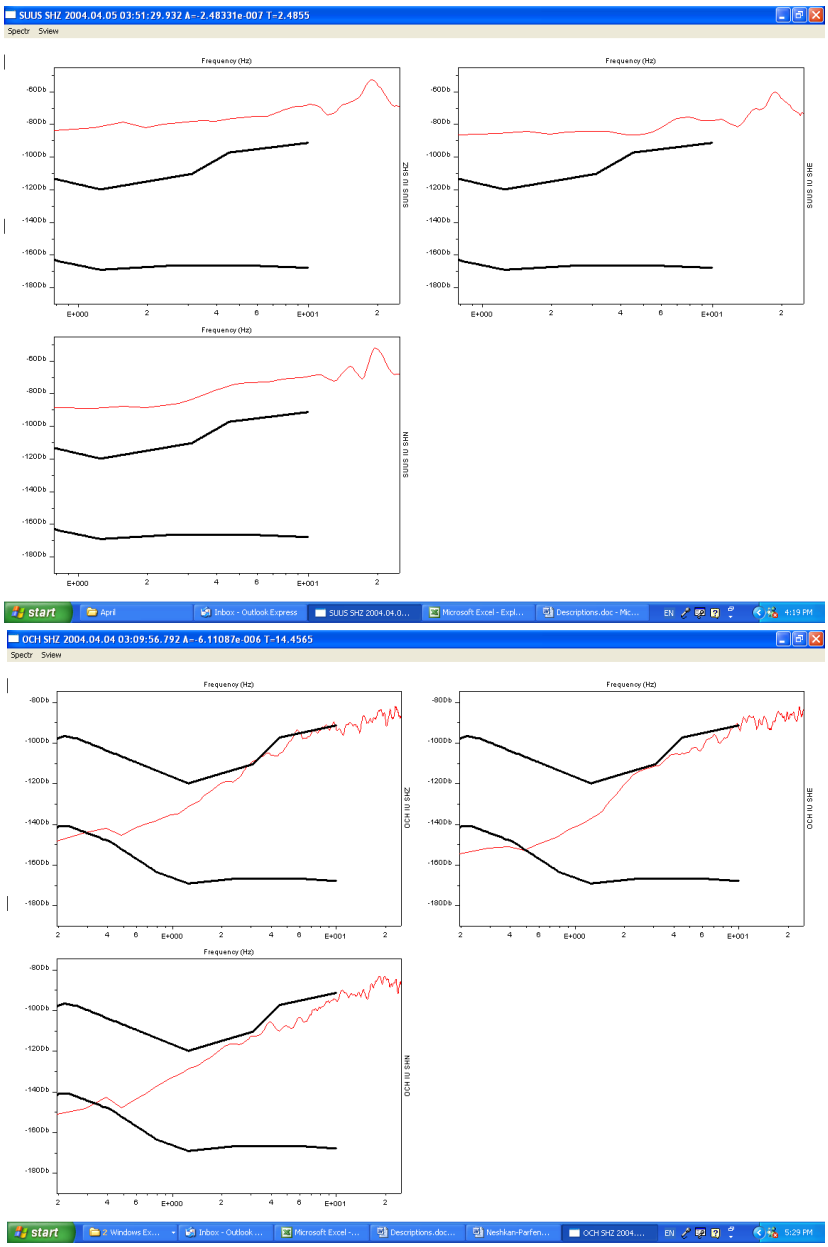

Figure 9. Top - Three component spectral amplitude plots for a mine explosion. Note that there is a dominant peak at 19-20 Hz that may result from a 50 ms delay between lines fired in the explosion. Bottom – a similar three-component spectral amplitude plot for a tectonic earthquake showing the absence of a 20 Hz peak.

REFERENCES

Linkimer, L. (2006). Discrimination of Earthquakes and Explosions in Eastern Russia by Amplitude Ratios Obtained from Analog Records. *MS Thesis*, Michigan State University, East Lansing, 180pp.

Mackey, K. G., H. Hartse, K. Fujita, L. Linkimer, L. Steck, R. Stead, and C. Rowe (2006). Seismic characterization of northeast Asia, in *Proceedings of the 28th Seismic Research Review: Ground-Based Nuclear Explosion Monitoring Technologies,* LA-UR-06-5471, Vol. 1, pp. 93–102.

Mackey, K. G., K. Fujita, L. V. Gounbina, B. M. Koz'min, V. S. Imaev, L. P. Imaeva, and B. M. Sedov, (2003). Explosion Contamination of the Northeast Siberian Seismicity Catalog: Implications for Natural Earthquake Distributions and the Location of the Tanlu Fault in Russia, *BSSA*, 93 (2): 737–746.

Rowe, C. A., W. S. Phillips, M. Maceira, M. L. Begnaud, L. K. Steck, X. Yang, C. L. Lucero, H. E. Hartse, R. J. Stead, K. Mackey, K. Fujita, and C. Ammon, (2007). Geophysical imaging of Asia and Siberia: Tomography for seismic velocity, upper mantle gradient, Lg attenuation, and joint inversion of surface wave dispersion, receiver functions and satellite gravity data, in current. Proceedings.

Zhang, H., K. G. Mackey, K. Fujita, L. Steck, C. Rowe, C. Thurber, and S. Roecker, (2007). High resolution three-dimensional seismic imaging of Baikal and Amur regions of eastern Russia, in current Proceedings.